RSC Advances

PAPER

View Article Online
View Journal | View Issue

Cite this: *RSC Adv.*, 2021, **11**, 1694

Bioinspired polymeric pigments to mimic natural hair coloring†

Yu Sun,[a] Congyu Wang,[a] Min Sun [a] and Zhen Fan *[ab]

Received 10th November 2020
Accepted 16th December 2020

DOI: 10.1039/d0ra09539g

rsc.li/rsc-advances

Due to an increasingly aging population, hair dyeing has become more necessary in daily life; however synthetic hair dyes often have the disadvantages of harsh dyeing conditions, a slow dyeing process and biological toxicity. Herein, we developed a bioinspired approach to mimic the natural hair dyeing process under mild conditions. Compared to the existing polydopamine deposition approach with harsh conditions, mild conditions and effective deposition were achieved here. First, in the presence of tyrosine hydroxylase and metal ions, dopamine could be oxidized into polydopamine, a mimic of human eumelanin, and then self-assembled into nanometer-scale pigments. Through optimizing the experimental parameters, various colors and the desired darkness could be achieved within less than 1 minute. In addition, significant durability was observed after continuous washing with polydopamine assemblies as hair dyes. Morphological analysis was applied to verify the deposition of polydopamine assemblies onto the hair surface, which induces the hair color change. Also, animal studies were conducted to evaluate the efficiency and biological toxicity of this approach. Overall, this bioinspired approach could provide a new avenue for biocompatible and effective nanomaterial-based hair dyes for at-home use.

Introduction

Human hair color is mainly determined by natural pigments named eumelanin, which are mostly distributed in the middle layer of human hair.[1–3] These pigments are organized into nanometer-scale particles,[4–7] and different ratios, concentrations, distributions and types of eumelanin lead to diverse hair colors. Eumelanin production is initiated by tyrosine hydroxylase, by which tyrosine is hydroxylated to L-dopa.[8–12] After the above initial reactions, L-dopa will be further oxidized to eumelanin. However, with increasing age, the production of eumelanin is reduced due to the lower antioxidant ability, higher oxidative stress,[13] and decreased pigment-forming melanocytes,[14] which induces the color loss of hair.

In ancient times, natural materials were used to pigment hair, such as black soya beans, vinegar and balsamine, the leaves of which can be made into a paste or powder that can dye hair a red or black color.[15] With the development of the modern chemical industry, synthetic hair dyes have been fabricated and released into the market since the 1900s.[16] Synthetic hair dyes are generally composed of three components: intermediates, couplers, and oxidants. Intermediates are usually aromatic amines that infiltrate into the keratin of hair, such as *p*-phenylenediamine, which is the most widely used intermediate of commercial hair dyes.[17] During the process of penetration, dye molecules are synthesized and attached to the hair. However, this kind of hair dye could cause certain damage to the human body. For example, *p*-phenylenediamine is one of the main causes of hair dye dermatitis.[18–21] According to existing studies of allergic reactions induced by *p*-phenylenediamine, 71.4% of the patients treated with *p*-phenylenediamine felt pruritus, 8.6% felt a prickling sensation and 1% felt a burning or tingling sensation.[21] In addition, it has been demonstrated that the use of synthetic hair colorants increases the risk of basal cell carcinoma, breast cancer and ovarian cancer.[22] However, minor progress has been made to avoid such defects of synthetic hair dyes.[21,23,24]

During the past decade, nanotechnology has provided novel approaches for new types of hair dyes.[25–28] In the first century AD, ancient Greek and Roman civilizations utilized PbS nanocrystals to pigment hairs.[29] Nowadays, nanoparticles, such as Au nanoparticles, Ag nanoparticles, and graphene nanosheets, have been developed as hair dyes. However, these methods also suffer from drawbacks such as a relatively slow rate of pigmentation, poor biocompatibility, impaired thermal insulation properties of hair, *etc.*[30–32] Therefore, a desirable approach could be the use of naturally occurring eumelanin nanoparticles to restore the color of hair fibers. However, existing protocols involving eumelanin require strong oxidative conditions,[33,34] which are not suitable for at-home applications.

[a]*Department of Polymeric Materials, School of Materials Science and Engineering, Tongji University, Shanghai 201804, China. E-mail: fanzhen2018@tongji.edu.cn*

[b]*Institute for Advanced Study, Tongji University, Shanghai 200092, China*

† Electronic supplementary information (ESI) available. See DOI: 10.1039/d0ra09539g

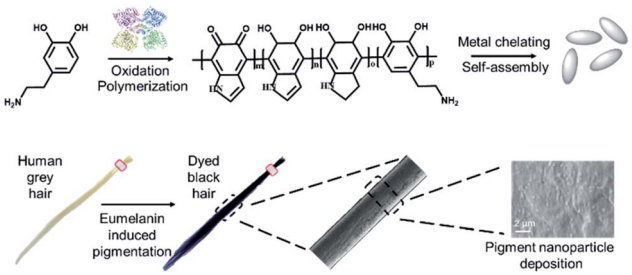

Scheme 1 A schematic illustration of the bioinspired synthesis of eumelanin mimetic polydopamine based pigments to mimic natural hair coloring.

Herein, we developed a bioinspired approach to synthesize eumelanin-mimetic nanoparticles and mimic the natural hair pigmentation process. As shown in Scheme 1, naturally occurring dopamine was first oxidized and polymerized to polydopamine using tyrosine hydroxylase. Afterwards, polydopamine self-assembled into nanoparticles and deposited onto the hair surface for pigmentation. Compared to the existing hair dyeing process, milder reaction conditions and more biocompatible molecules were applied here. Through optimizing the experimental parameters, the desired hair color and darkness could be achieved. In addition, due to the high catalytic efficiency of tyrosine hydroxylase, the whole dyeing process could be completed in less than one minute. Besides human hair, mice were also tested to confirm the dyeing capability of the polydopamine assemblies. In comparison with commercial hair dye, our approach could achieve similar effects with a shorter reaction time and no biohazardous waste.

Experimental

Materials

Dopamine hydrochloride was purchased from Inno-chem Co., Ltd. Tyrosine hydroxylase was purchased from Sigma-Aldrich (China). Iron chloride hexahydrate ($FeCl_3 \cdot 6H_2O$), iron sulfate heptahydrate ($FeSO_4 \cdot 7H_2O$) and copper sulfate pentahydrate ($CuSO_4 \cdot 5H_2O$) were purchased from Aladdin Co., Ltd. To test the hair dyeing ability of our method, grey hair samples were purchased from Narcissus Salon. BALB/c mice were purchased from the Institutional Animal Care and Shanghai Slaccas Laboratory Animals Co., Ltd.

Hair dyeing

Hair samples were randomly divided into groups and cut into 2 cm lengths for further experiments. 2 mL of dopamine hydrochloride (5 mg mL^{-1}) was added into a centrifuge tube and hair samples (10 mg) were then immersed in it. Afterwards, 60 μL of tyrosine hydroxylase (7 mg mL^{-1}) was added into the mixture solution of hair and dopamine hydrochloride. Then, 0.5 mL aqueous solution of the metal chelators were added (10 mmol L^{-1} $FeCl_3$, 10 mmol L^{-1} $FeSO_4$ or 10 mmol L^{-1} $CuSO_4$). The dyeing process was carried out at room temperature. After five minutes of dyeing, all the hair samples were washed with water five times and air-dried at room temperature.

Characterization of the polydopamine assemblies

The polydopamine assemblies synthesized above were diluted 20 times and UV-visible (UV-vis) absorption spectra were recorded by an ultraviolet spectrophotometer from Shanghai Jingke. 10 μL of the diluted solution dripped onto a nitrocellulose-covered copper grid, which was then air-dried. TEM was carried out by a JEOL JEM-2100F instrument at 200 kV equipped with a Gatan 894 Ultrascan 1 k CCD camera. 10 μL of the diluted solution was dripped onto a silicon wafer substrate. Afterwards, SEM was applied to characterize the morphology of the polydopamine assemblies and hair after dyeing. 3 mL of the dyeing solution was freeze dried by Scientz-12N. Afterwards, the freeze-dried powder was characterized using an infrared spectrometer (Nicolet iS5). The dyed hair was cut into short lengths and then analysed by FTIR-ATR spectroscopy. Dyed hair samples were soaked in water for 2 minutes and then air-dried at room temperature. The hair samples were cut into 5–7 mm lengths and adhered onto the SEM sample stage with conductive tape. After lightly pressing, the SEM images were taken by a scanning electron microscope from Zeiss.

Quantitative analysis of hair color

Hair color intensity was analyzed by a previous method using ImageJ.[33] One fixed size area in the digital image was randomly selected and its RGB value ($I = I_R + I_G + I_B$) was calculated through ImageJ. Grey hair acted as the control experiment background (I_0). The darkness (D) was calculated as $D = (I_0 - I)/I_0$. The RGB color ratio was analyzed using ImageJ through RGB Measure Plugins in order to differentiate the colors from different conditions.

Characterization of mechanical properties

The tensile tests were performed with MTS exceed model E42 with a gauge length of 15 mm at a loading rate of 10 mm min^{-1}. Stress–strain curves were recorded as an average of three different samples.

Characterization of the loading amount of metal ions

Hair samples were randomly divided into groups and cut into 2 cm lengths for further experiments. 120 μL of the tyrosine hydroxylase (7 mg mL^{-1}) and 1 mL of the metal solution (10 mM) were added into 4 mL of the dopamine solution (5 mg mL^{-1}) in sequence. Afterwards 280 mg of hair was added into each kind of dyeing solution mixture solution for the dyeing process. The dyeing process was carried out at room temperature. After five minutes, the resultant solution was collected and its metal concentration was analyzed using a PinAAcle 900T atomic absorption spectrometer.

Animal experiments

All procedures were approved by the Tongji University Animal Studies Committee. Overall care of the animals was consistent with the Guide for the Care and Use of Laboratory Animals from the National Research Council and the USDA Animal Care Resource Guide. Female mice bred freely for 1 week, and then their backs were shaved to expose the fur below. For toxicity analysis, 1 mL of the aqueous dyeing solution was dropped onto the backside of the nude mice and air-dried at room temperature. To evaluate the toxicity, the skin conditions of the treated mice were observed for a week. For the hair dyeing, 1 mL of the solution was dripped onto their backs and then smeared evenly with clear gloves. Five minutes later, photographs were taken.

Results and discussion

Preparation and characterization of the PDA assemblies

Under the catalysis of tyrosinase hydroxylase, dopamine was first oxidized and polymerized to dopaquinone. Following the 1,4-Michael addition of dopamine, leucodopaminechrome was formed through intramolecular cyclization and then oxidized to dopaminechrome, which was further polymerized to polydopamine.[35] In addition, metal ions were also applied to induce the self-assembly of polydopamine and immobilize the pigment nanoparticles onto the hair surface.[33] Specifically, $FeCl_3$, $FeSO_4$ and $CuSO_4$ aqueous solutions were introduced into the polydopamine assemblies. UV-vis spectra of the polydopamine assemblies with various metal ions were recorded (Fig. 1a and S1†). The absorbance at 280 nm was derived from the transition of dopamine La–Lb, which was characteristic of the intraligand π–π* transition. The absorbance at 308 nm corresponded to semiquinone, which may come from dopaquinone, leucodopaminechrome or polydopamine.[36–38]

The FT-IR spectra also provided evidence for oxidation and polymerization. Fig. 1b showed obvious differences between dopamine before and after treatment. The absorbance at around 1728 cm^{-1} was derived from the stretching vibration of the C=O group, which was formed by oxidation of catechol.[39,40] It indicated the formation of polydopamine from dopamine. Besides new absorbance in the UV-vis and FT-IR spectra, the formation of diverse chromophore structures can be indicated from the coloration of a dopamine aqueous solution treated with tyrosine hydroxylase (Fig. 1c). The color variation could be attributed to different types of self-assembled nanoparticles owing to the selections of metal ions. Meanwhile, the nanomorphologies of the polydopamine assemblies were characterized using TEM and SEM (Fig. 1d, e, S2 and S3†). As shown in Fig. 1d and e, rice-shaped nanoparticles were observed of polydopamine assemblies with Fe^{3+} chelation, which share a similar morphology to natural eumelanin granules.[4]

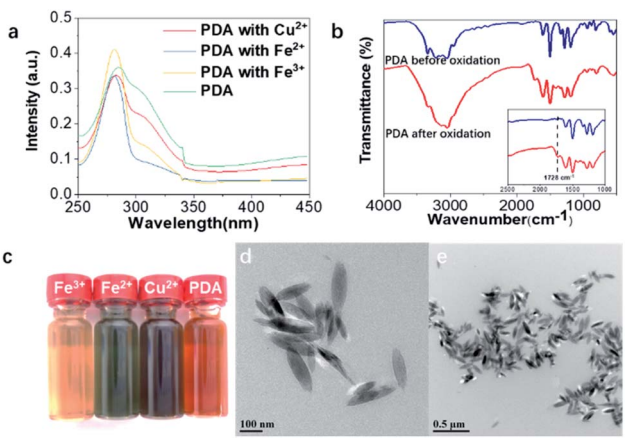

Fig. 1 Characterization of polydopamine assemblies. (a) UV-vis spectra. (b) FT-IR spectra of polydopamine chelated with various metal ions. (c) Polydopamine assemblies under various experimental conditions. (d and e) TEM images of polydopamine assemblies with Fe^{3+} ions.

Hair dyeing with PDA assemblies

To evaluate the hair dyeing capability, human grey hair was purchased and dyed with polydopamine assemblies. Human hair samples were cut into fragments approximately 3 cm long and then placed into a 5 mL centrifuge tube. Then, aqueous solutions of dopamine, tyrosine hydroxylase and metal ions were added in sequence at room temperature. Within less than one minute, hair samples treated with dopamine and metal ions (Fe^{3+}, Fe^{2+}, Cu^{2+} and without metal ions) displayed significant color changes (Fig. 2a). Both color change and darkening could be observed from the hair after dyeing. To further quantitatively evaluate the dyeing efficiency, the darkness and RGB ratio were analyzed using the existing protocol.[33] As shown in Fig. 2c, hair darkness could be tuned by the choice of metal ions, which suggested that Fe^{3+} ions possess the strongest chelating ability for hair dyeing. To evaluate the loading amount of metal ions to the hair, atomic absorption

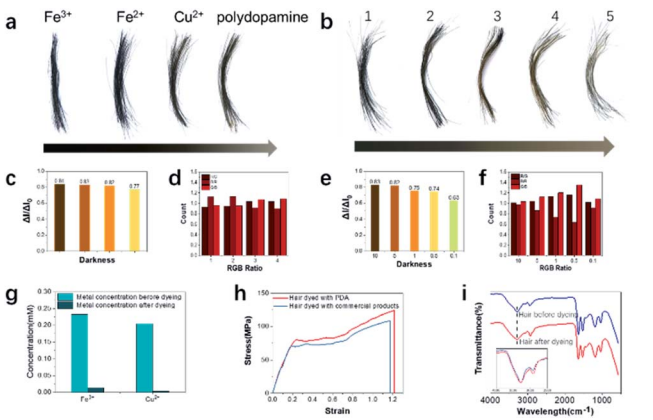

Fig. 2 Various hair color and darkness after dyeing with polydopamine assemblies. (a) Images of hair samples after dyeing with polydopamine assemblies chelating with Fe^{3+}, Fe^{2+}, Cu^{2+} and pure polydopamine. (b) Images of hair samples dyed with polydopamines of various Fe^{3+} ions concentrations: (1) 10 mM, (2) 5 mM, (3) 1 mM, (4) 0.5 mM, and (5) 0.1 mM. (c and e) Variations in the RGB intensity of images of the hair samples (a and b). (d and f) RGB color ratios of the hair samples (a and b). (g) Consumption of different metal ions during the hair dyeing process. (h) The stress–strain curves of different hair samples. (i) FTIR-ATR spectra of hair before and after the dyeing process.

spectrometry analysis was conducted. As shown in Fig. 2g, the highest loading amount occurred to Fe^{3+}, which was consistent with its best dyeing performance due to the enhanced coordination ability.

In addition, compared to the other metal ions applied here, Fe^{3+} ions had considerable oxidative ability and could participate in the intramolecular oxidation of dopamine, resulting in enhanced hair dyeing capacity.[41] Besides the darkening variation, different colors from brown to black were obtained after treatment with polydopamine with metal ions (Fig. 2a and d). To quantitatively differentiate the detailed color, the RGB ratios of hair samples after dyeing were also analyzed, suggesting that both polydopamine with Fe^{2+} and Fe^{3+} produced a black color after dyeing of grey hair. Due to the most effective hair dyeing being achieved by using polydopamine with Fe^{3+} ions, this protocol was further explored. Various concentrations of Fe^{3+} ions were applied to optimize the dyeing effects. As shown in Fig. 2b, the hair color changed from brown to black with increase concentrations of Fe^{3+} ions. To explore the hair quality after dyeing, the mechanical properties characterization was conducted. Clear differences between the hair samples were observed in the stress–strain curve. Compared with the commercial product dyed hair, the PDA dyed hair had a higher elongation at break and breaking stress, which indicated that the PDA dyeing hair could achieve a large strain under high stress with better toughness. Meanwhile the Young's modulus of PDA dyed hair was lower than the commercial product dyed hair. It showed the poor ability of resistance to deformation, which also indicated its good softness. Compared to hair dyed with commercial product, the stress–strain curves indicated that hair after PDA dyeing demonstrated better toughness and softness.[42,43] Fig. 2i suggested that the hair was rarely changed before and after dyeing. The broad peak at 3280 cm^{-1} was due to the stretching vibration of N–H. The wider peak after dyeing in this area was due to the linkage structure (hydrogen bond) between the hair and polydopamine assemblies.[44] There were small changes located in the amide I and amide II band regions (1690–1600 cm^{-1} and 1575–1480 cm^{-1}, respectively), resulting from overlapping between the hair and polydopamine bands.[16] These results indicate that our bioinspired approach could develop a eumelanin-mimic natural pigment to mimic natural hair pigmentation with a desired color and darkness without harsh conditions or strong oxidants.

Optimization of the hair dyeing process

After initial exploration, the concentration of tyrosine hydroxylase and reaction time were further optimized to study their effects on hair dyeing. Hair color changed from brown to black with increasing enzyme concentration (Fig. 3a). Similarly, the darkness and RGB ratio of the treated hair were analyzed (Fig. 3d and g). It was indicated that the oxidation process would also affect the darkness and color of the treated hair, which could be manipulated through adjusting the concentration of tyrosine hydroxylase. In addition, the dyeing efficiency of the polydopamine assemblies was also studied with various reaction time. As shown in Fig. 3b, the hair samples became black after treatment with polydopamine

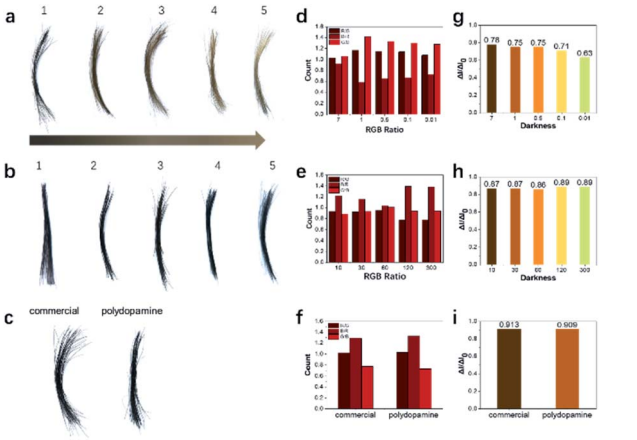

Fig. 3 Hair color and darkness after tuning enzyme concentration and reaction time. (a) Images of hair samples treated with various concentrations of tyrosine hydroxylase during the dyeing process: (1) 7 mg mL^{-1}, (2) 1 mg mL^{-1}, (3) 0.5 mg mL^{-1}, (4) 0.1 mg mL^{-1}, and (5) 0.01 mg mL^{-1}. (b) Images of hair samples after dyeing with various periods of time: (1) 10 s, (2) 30 s, (3) 60 s, (4) 120 s, and (5) 300 s. (c) Images of hair samples after dyeing with commercial hair dyes (left) and polydopamine based pigments (right). (d–f) Variations in the RGB intensity of images of hair samples (a–c). (g–i) RGB color ratios of the hair samples shown in (a–c).

assemblies for 10 seconds, which was significantly faster than existing protocols and commercial dyes.[16,17,33,34,45,46] Furthermore, no obvious difference was observed from the darkness of the hair samples after various reaction times, indicating a significantly high efficiency. This could be attributed to the high catalytic efficiency of tyrosine hydroxylase and the chelating capability of metal ions during the dyeing process. After confirming the dyeing capability of polydopamine assemblies, commercial hair dye was introduced here for comparison. As shown in Fig. 3c, similar hair color and darkness were observed visually after dyeing with these two pigments. Besides visual inspection, the RGB ratio and color intensity of the hair images also indicated similar results (Fig. 3f and i). After washing with shampoo five times, both hair color and darkness remained similar. However, compared to the turbid water, the wastewater after washing of the hair treated with polydopamine assemblies remained clear, indicating a more biocompatible and biofriendly dyeing process (Fig. S4†). In addition, to further evaluate the biocompatibility and dyeing efficiency of this approach, BALB/c mice were used here as the animal model for dyeing and cytotoxicity tests. A clear hair color change was observed after treatment with polydopamine assemblies (Fig. S5†). No significant adverse symptoms were discovered before and after treatment with dyeing solution for one week (Fig. S6†), which confirmed the biocompatibility of the polydopamine assemblies. Also, no obvious allergic or toxic reactions were discovered during the two-week animal experiments.

The mechanism study of the PDA assemblies deposition

The pigment deposition during the hair dyeing process was also studied using SEM before and after dyeing with washing 5 times. Compared to the hair before dyeing (Fig. 4a), hair treated

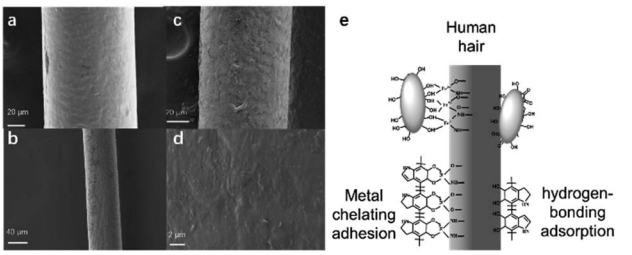

Fig. 4 Deposition analysis of polydopamine assemblies on the surface of human hair. SEM images of natural human grey hair before dyeing and after dyeing with polydopamine assemblies (a–d), indicating nanometer-sized pigments deposited on the surface of hair after washing. (e) A scheme showing the possible mechanism of polydopamine assemblies deposited onto the hair surface.

with the polydopamine assemblies seemed to have a rougher surface (Fig. 4b–d), which could be attributed to the deposition of pigments. Although similar depositions were also discovered in existing reports of utilizing dopamine as a hair dye,[16,33,34] most of these methods demanded an alkali environment and/or a strong oxidizing agent like H_2O_2 to achieve hair dyeing. As shown in Fig. S6a and b,† clear hair damage could be observed from SEM images after treatment with NaOH or H_2O_2. This strong attachment between the polydopamine nanoparticles and the hair surface could be attributed to the unique chemophysical properties of polydopamine and the chelating ability of metal ions.[47,48] Keratin as the main surface component of hair has abundant carboxyl, amino and hydroxyl groups,[1,49] which could form numerous hydrogen bonds with the catechol and amine groups of polydopamine.[50–52] In addition, metal ions could play key roles in chelating with polydopamines and also with the keratin of the human hair surface.[16,33,34] As shown in Fig. 4e, the strong deposition could be attributed to the network of hydrogen bonds and metal chelation between the hair and polydopamine nanoparticles.

Conclusions

In conclusion, we developed a bioinspired approach to mimic the natural hair dyeing process under mild conditions. In the presence of tyrosine hydroxylase and metal ions, dopamine could be oxidized into polydopamine, a mimic of human eumelanin, and then self-assembled into nanometer-scale pigments. Afterwards, by metal chelation and hydrogen bond adsorption, the polydopamine assemblies could be deposited onto the hair surface. Through optimizing the experimental parameters, various colors and the desired darkness could be achieved within less than 1 minute. Compared to existing polydopamine deposition approaches with harsh conditions, mild conditions and effective deposition were achieved here. Our experimental results suggest that this bioinspired approach could pave an alternative and effective path for at-home hair dyes.

Conflicts of interest

There are no conflicts to declare.

Acknowledgements

This research was supported by the National Natural Science Foundation of China (No. 51803152) and the Natural Science Foundation of Shanghai (No. 19ZR1478800).

Notes and references

1 M. Cetin, E. Bozbeyoglu, T. Erdogan, S. A. Kocaman, O. Satiroglu and M. E. Durakoglugil, *North. Clin. Istanb.*, 2019, **6**, 33–36.
2 J. P. Ortonne and G. Prota, *J. Invest. Dermatol.*, 1993, **101**, S82–S89.
3 A. C. Santos Nogueira and I. Joekes, *J. Photochem. Photobiol., B*, 2004, **74**, 109–117.
4 S. Ghiani, S. Baroni, D. Burgio, G. Digilio, M. Fukuhara, P. Martino, K. Monda, C. Nervi, A. Kiyomine and S. Aime, *Magn. Reson. Chem.*, 2008, **46**, 471–479.
5 Q. Fan, K. Cheng, X. Hu, X. Ma, R. Zhang, M. Yang, X. Lu, L. Xing, W. Huang, S. S. Gambhir and Z. Cheng, *J. Am. Chem. Soc.*, 2014, **136**, 15185–15194.
6 Y. Liu, K. Ai, J. Liu, M. Deng, Y. He and L. Lu, *Adv. Mater.*, 2013, **25**, 1353–1359.
7 Y. Liu, K. Ai, X. Ji, D. Askhatova, R. Du, L. Lu and J. Shi, *J. Am. Chem. Soc.*, 2017, **139**, 856–862.
8 C. Giulivi, N. J. Traaseth and K. J. Davies, *Amino Acids*, 2003, **25**, 227–232.
9 P. M. Plonka and M. Grabacka, *Acta Biochim. Pol.*, 2006, **53**, 429–443.
10 V. D. Marmol and F. Beermann, *FEBS Lett.*, 1996, **381**, 165–168.
11 C. Giulivi and K. J. Davies, *J. Biol. Chem.*, 2001, **276**, 24129–24136.
12 Z. Li, T. Wang, F. Zhu, Z. Wang and Y. Li, *Chin. Chem. Lett.*, 2020, **31**, 783–786.
13 M. Cetin, E. Bozbeyoglu, T. Erdogan, S. A. Kocaman, O. Satiroglu and M. E. Durakoglugil, *North. Clin. Istanb.*, 2019, **6**, 33–39.
14 J. E. Kim, H. D. Jung and H. Kang, *Ann. Dermatol.*, 2012, **24**, 274–279.
15 G. S. Gozubuyuk, E. Aktas and N. Yigit, *J. Mycol. Med.*, 2014, **24**, 313–318.
16 C. Battistella, N. C. McCallum, K. Gnanasekaran, X. Zhou, V. Caponetti, M. Montalti and N. C. Gianneschi, *ACS Cent. Sci.*, 2020, **6**, 1179–1188.
17 J. K. Lee, H. E. Lee, G. Yang, K. B. Kim, S. J. Kwack and J. Y. Lee, *Toxicol. Res.*, 2020, **36**, 329–336.
18 I. E. Lopez, J. E. Turrentine and P. D. Cruz, Jr, *Dermatitis*, 2014, **25**, 32–33.
19 D. Patel, S. Narayana and B. Krishnaswamy, *Int. J. Trichol.*, 2013, **5**, 140–143.
20 J. D. Svalgaard, C. Saermark, M. Dall, K. Buschard, J. D. Johansen and K. Engkilde, *Immunol. Res.*, 2014, **58**, 40–50.
21 J. H. Han, H. J. Lee, C. H. Bang, J. H. Lee, Y. M. Park and J. Y. Lee, *Ann. Dermatol.*, 2018, **30**, 316–321.

22 Y. Zhang, B. M. Birmann, J. Han, E. L. Giovannucci, F. E. Speizer, M. J. Stampfer, B. A. Rosner and E. S. Schernhammer, *BMJ*, 2020, **370**, m2942.
23 M. Kock, P. J. Coenraads, B. Blomeke and C. Goebel, *Br. J. Dermatol.*, 2016, **174**, 1042–1050.
24 O. J. Morel and R. M. Christie, *Chem. Rev.*, 2011, **111**, 2537–2561.
25 M. Ferrari, *Nat. Rev. Cancer*, 2005, **5**, 161–171.
26 D. R. Paul and L. M. Robeson, *Polymer*, 2008, **49**, 3187–3204.
27 M. Sarikaya, C. Tamerler, A. K. Y. Jen, K. Schulten and F. Baneyx, *Nat. Mater.*, 2003, **2**, 577–585.
28 D. V. Talapin and E. V. Shevchenko, *Chem. Rev.*, 2016, **116**, 10343–10345.
29 P. Walter, E. Welcomme, P. Hallegot, N. J. Zaluzec, C. Deeb, J. Castaing, P. Veyssiere, R. Breniaux, J. L. Leveque and G. Tsoucaris, *Nano Lett.*, 2006, **6**, 2215–2219.
30 S. D. Haveli, P. Walter, G. Patriarche, J. Ayache, J. Castaing, E. Van Elslande, G. Tsoucaris, P. A. Wang and H. B. Kagan, *Nano Lett.*, 2012, **12**, 6212–6217.
31 D. S. Im, B. M. Hong, M. H. Kim and W. H. Park, *Colloids Surf., A*, 2020, **600**, 124995.
32 C. Luo, L. Zhou, K. Chiou and J. Huang, *Chem*, 2018, **4**, 784–794.
33 Z. F. Gao, X. Y. Wang, J. B. Gao and F. Xia, *RSC Adv.*, 2019, **9**, 20492–20496.
34 K. M. Im, T.-W. Kim and J.-R. Jeon, *ACS Biomater. Sci. Eng.*, 2017, **3**, 628–636.
35 Q. Wei, F. Zhang, J. Li, B. Li and C. Zhao, *Polym. Chem.*, 2010, **1**, 1430.
36 W. J. Barreto, S. R. Barreto, R. A. Ando, P. S. Santos, E. DiMauro and T. Jorge, *Spectrochim. Acta, Part A*, 2008, **71**, 1419–1424.
37 J.-J. Feng, P.-P. Zhang, A.-J. Wang, Q.-C. Liao, J.-L. Xi and J.-R. Chen, *New J. Chem.*, 2012, **36**, 148–154.
38 E. Mazario, J. Sánchez-Marcos, N. Menéndez, P. Herrasti, M. García-Hernández and A. Muñoz-Bonilla, *RSC Adv.*, 2014, **4**, 48353–48361.
39 N. B. Sanches, R. Pedro, M. F. Diniz, E. D. C. Mattos, S. N. Cassu and R. d. C. L. Dutra, *J. Aerosp. Technol. Manage.*, 2013, **5**, 421–430.
40 K. Forfang, B. Zimmermann, G. Kosa, A. Kohler and V. Shapaval, *PLoS One*, 2017, **12**, e0170611.
41 P. Qi, D. Zhang and Y. Wan, *Talanta*, 2017, **170**, 173–179.
42 A. Franbourg, P. Hallegot, F. Baltenneck, C. Toutain and F. Leroy, *J. Am. Acad. Dermatol.*, 2003, **48**, S115–S119.
43 Y. Yu, W. Yang, B. Wang and M. A. Meyers, *Mater. Sci. Eng., C*, 2017, **73**, 152–163.
44 Y. Ding, J. Wang and S. Song, *Polymers*, 2020, **12**, 1–15.
45 H. Geng, L. Zhuang, M. Li, H. Liu, F. Caruso, J. Hao and J. Cui, *ACS Appl. Mater. Interfaces*, 2020, **12**, 29826–29834.
46 M. Rincón-Fontán, L. Rodríguez-López, X. Vecino, J. M. Cruz and A. B. Moldes, *RSC Adv.*, 2017, **7**, 16444–16452.
47 H. Lee, S. M. Dellatore, W. M. Miller and P. B. Messersmith, *Science*, 2007, **318**, 426–430.
48 Q. Ye, H. Wang, B. Yu and F. Zhou, *RSC Adv.*, 2015, **5**, 60090–60095.
49 C. F. Cruz, M. Martins, J. Egipto, H. Osório, A. Ribeiro and A. Cavaco-Paulo, *RSC Adv.*, 2017, **7**, 51581–51592.
50 S. Hong, J. Yeom, I. T. Song, S. M. Kang, H. Lee and H. Lee, *Adv. Mater. Interfaces*, 2014, **1**, 1400113.
51 M. E. Lynge, R. van der Westen, A. Postma and B. Stadler, *Nanoscale*, 2011, **3**, 4916–4928.
52 M. Rahimnejad and W. Zhong, *RSC Adv.*, 2017, **7**, 47380–47396.